ELSEVIER

Remote Estimation of Water Clarity in Optically Complex Estuarine Waters

Dana L. Woodruff, Richard P. Stumpf,† Julie A. Scope,* and Hans W. Paerl‡*

AVHRR satellite imagery was evaluated as a potential data source for monitoring light attenuation (K_{PAR}), as a measure of turbidity, in Pamlico Sound estuary, North Carolina. In situ *water quality data and reflectance imagery collected on 10 different dates were used to calibrate a general optical equation relating satellite-derived reflectance (R_d), nominally $R_{(630\ nm)}$ to K_{PAR}. Additional spectral data (e.g., absorption, subsurface reflectance), related reflectance and K_{PAR} to changes in phytoplankton pigments, organic matter, and suspended sediments. Optically, Pamlico Sound, North Carolina is dominated by scattering from suspended sediments, whereas the tributary rivers are dominated by absorption from both dissolved and particulate organic matter. A general relationship developed between R_d and K_{PAR} ($r^2=0.72$) in Pamlico Sound was found useful in a variety of environmental conditions; however a relationship between R_d and suspended sediment concentration was less robust, and affected by changing sediment characteristics. In the rivers, high and variable absorption in the visible wavelengths precluded development of a relationship between R_d and K_{PAR}. The relationship developed between R_d and K_{PAR} in Pamlico Sound is similar to those determined for Delaware Bay and Mobile Bay in previous studies, suggesting possible broader regional application of algorithms for coastal bays and estuaries having similar sediment characteristics, with direct application to SeaWiFS data. Published by Elsevier Science Inc.*

* NOAA/National Marine Fisheries Service, Beaufort, North Carolina

† U.S. Geological Survey/Center for Coastal Geology, St. Petersburg, Florida

‡ Institute of Marine Sciences, University of North Carolina, Morehead City

Address correspondence to Dana Woodruff, Battelle Marine Sciences Laboratory, 1529 West Sequim Bay Rd., Sequim, WA, 98382. E-mail: dana.woodruff@pnl.gov

Received 3 July 1996; revised 10 November 1998.

INTRODUCTION

Concerns about increased turbidity and associated ecological impacts in estuarine and coastal waters have prompted recent efforts to relate satellite observations to *in situ* properties of light attenuation in the water column (Stumpf and Pennock; 1991). Remote sensing techniques offer the ability to synoptically characterize large-scale trends and variability of water quality parameters. Remote quantification of light attenuation has focused on oceanic regions (Smith and Baker, 1978; Morel, 1988; Spinrad, 1989; Platt et al., 1991) owing to the relative optical simplicity of oceanic waters and the past availability of Coastal Zone Color Scanner (CZCS) data, which had limited application in estuaries. Light attenuation in oceanic (Case I) waters (Morel and Prieur, 1977; Gordon and Morel, 1983) is due primarily to phytoplankton pigments and their derivative products (not including water) (Smith and Baker, 1978). Case II (coastal) waters and estuaries contain significant quantities of terrigenous material which results in greater optical complexity in the form of inorganic particulates, and a greater variety and higher concentration of dissolved and particulate organic matter.

Empirically derived calibration algorithms from remotely sensed reflectance data provide site-specific predictions of water quality parameters with reasonable accuracy, but are limited in their universal application (Austin and Petzold, 1981; Whitlock et al., 1981; Khorram, 1985; Khorram and Cheshire, 1985; Gould and Arnone, 1997). A more rigorous approach is the development of semi-analytic models which employ solutions to the radiative transfer equation for deriving absorption and scattering coefficients. Such models allow remote sensing measurements to be understood in terms of the inherent optical characteristics, and provide insight into the characteristics of the effectiveness and significance of differences in algorithm coefficients in various regions.

REMOTE SENS. ENVIRON. 68:41–52 (1999)
Published by Elsevier Science Inc.
655 Avenue of the Americas, New York, NY 10010

0034-4257/99/$–see front matter
PII S0034-4257(98)00108-4

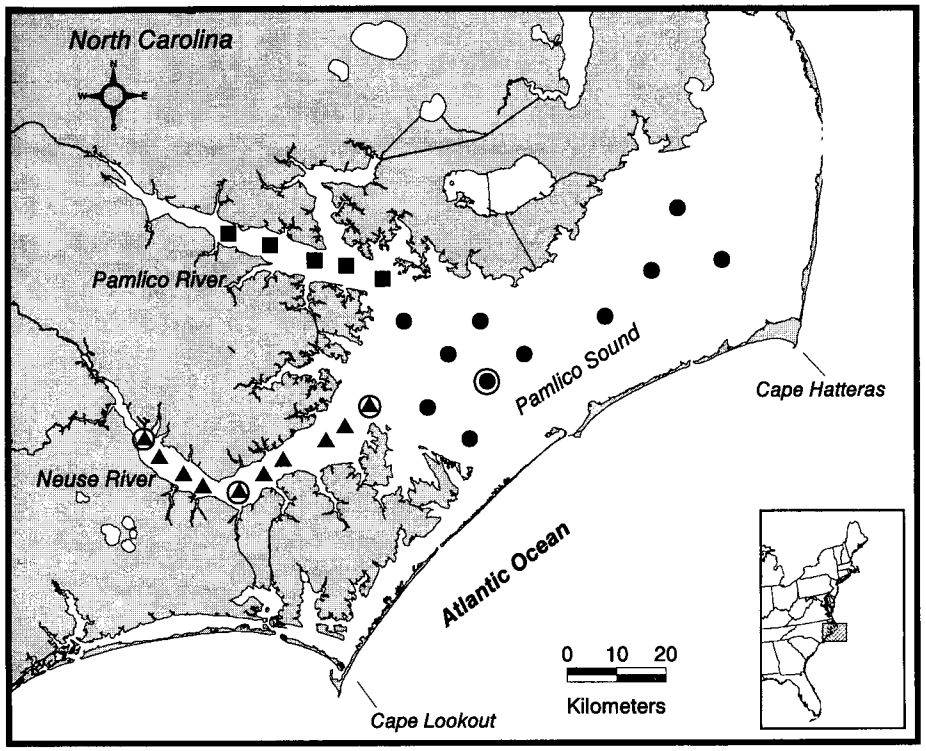

Figure 1. Location of sampling stations in the Neuse River (▲), Pamlico River (■), and Pamlico Sound (●) between 1991 and 1993. Circled stations were sampled for in-water reflectance and inherent optical properties in 1994.

A modification of the Gordon et al. (1975) solution of the radiative transfer equation was applied by Stumpf and Pennock (1989; 1991), which equates visible reflectances to measurements of suspended sediments and light attenuation in estuarine waters, with application to AVHRR. In this study we present further applications of that algorithm to Pamlico Sound and its tributaries in North Carolina, define the geographic limitation of the model within our study area based on optical characteristics of the water, and examine variations over time within our data set.

The AVHRR, while not designed as an ocean color instrument, has particular utility even with the recent launch of SeaWiFS. The sensor offers a 15-year data set that can be used to describe trends in light attenuation in coastal zones. The AVHRR has demonstrated changes in Florida Bay over 12 years (Stumpf and Frayer, 1997). Its projected continuation into the future and daily coverage (versus 2-day coverage for SeaWiFS), will permit integration of these two sensors into the future.

Study Area

The Pamlico Sound estuarine complex is a coastal lagoon separated from the Atlantic Ocean by barrier islands (Fig. 1). The sound is relatively shallow (mean depth 5 m, typically 2–8 m at more than 2 km from shore) with predominantly wind-driven circulation (Epperly and Ross, 1986). The Neuse and Pamlico rivers originate in the Piedmont area of North Carolina and discharge directly into western Pamlico Sound. Collectively, they drain over 26,000 km^2, with the watershed comprised of approximately 64% forest, 24% agricultural land, and 3% urban area. Average discharge rates for the Neuse and Pamlico rivers are modest: 173 m^3 s^{-1} and 154 m^3 s^{-1}, respectively (Epperly and Ross, 1986). Numerous streams and embayments collect overland runoff from the extensive low-lying wetlands characteristic of eastern North Carolina, contributing to an increase of organic matter in the rivers. The region has been impacted by accelerated eutrophication, partially caused by increased urbanization, agricultural runoff, sewage discharge, and groundwater and atmospheric pollutant inputs (Copeland and Gray, 1989; Paerl et al., 1995). A majority of nutrient loading, particularly nitrogen, occurs during high-flow, winter-spring periods (Paerl et al., 1995; 1998). Periodic nutrient pulses, coupled with increased river discharge, cause shifts in phytoplankton composition and biomass, and primary productivity in the estuary (Mallin et al., 1991; Pinckney et al., 1998; Paerl et al., 1998). Thus, the factors causing increased light attenuation (organic matter, phytoplankton, and suspended sediments) vary temporally as well as spatially.

Theory

The model used in this study is derived from the Gordon et al. (1975) solution to the radiative transfer equation which allows reflectance from the water column, an apparent optical property, to be described in terms of its inherent optical properties, absorption (a) and backscatter (b_b). For an optically-deep (<10% of surface radiance

reaching the bottom), vertically homogeneous water column, reflectance is expressed as [Eq. (1)]

$$R_w(\lambda) \equiv \frac{E_u(\lambda)}{E_d(\lambda)} = Y \frac{b_b(\lambda)}{a(\lambda)+b_b(\lambda)}, \quad (1)$$

where R_w is the irradiance reflectance just below the water's surface, λ is the spectral band, E_u is upwelling irradiance, E_d is downwelling irradiance, b_b is the backscatter coefficient, a is the absorption coefficient and Y is a constant (0.33) (Gordon et al., 1975). In Case I waters and clearer Case II waters, backscatter is much less significant than absorption and $R_w(\lambda)$ can be described as $b_b(\lambda)/a(\lambda)$.

Stumpf and Pennock (1989) modified Eq. (1) for use in Case II waters, to estimate suspended sediment concentrations in Delaware Bay, a moderately turbid estuary. Since diffuse light attenuation (K_{PAR}) correlated strongly with suspended sediment concentration in this estuary (Pennock, 1985; Stumpf and Pennock, 1991), Stumpf and Pennock (1991) were able to modify the equation to develop a predictive model for K_{PAR} from R in the logistic form of [Eq. (2)]

$$R(\lambda) = \frac{Y'F(\lambda)}{(1+G(\lambda)/K_{PAR}(\lambda))}, \quad (2)$$

where R is remotely sensed (above-water) reflectance, and Y' is equal to 0.178 which incorporates Y from Eq. (1) and surface refraction and reflection effects. F represents a term for scattering and G an absorption term, both of which can be determined through regression analysis (Stumpf and Pennock, 1991). This relationship was derived assuming that attenuation is correlated to backscatter, resulting from increased suspended sediments. The AVHRR Band 1 lies outside the region of major pigment absorption peaks. Therefore, in turbid waters reflectance will generally increase with K_{PAR} (assuming a fixed absorption term) due to increased backscattering.

Satellite reflectance $R(\lambda)$ as used here is related to normalized water-leaving radiance $[L_w(\lambda)]_N$ (Gordon et al., 1983) or remote sensing reflectance R_{RS} (Carder and Steward, 1985) through [Eq. (3)]

$$\frac{Q[L_w(\lambda)]_N}{E_0} \equiv QR_{RS}(\lambda) = R(\lambda) = \frac{QL_w(\lambda)}{E_d(\lambda)}, \quad (3)$$

where L_w is the water-leaving radiance above the surface, E_0 is the extraterrestrial solar irradiance, and E_d is downwelling irradiance. Q is a factor relating upwelled radiance to irradiance and is set nominally to π, which assumes a Lambertian reflector. Q may vary (Morel and Gentili, 1993; Morel et al., 1995), the exact value important for determining inherent optical properties.

As a measure of water clarity, the diffuse attenuation coefficient (K_{PAR}) for photosynthetically active radiation (PAR) between 400 nm and 700 nm is fundamental for phytoplankton and seagrass production and growth studies in coastal areas. The exponential rate of light decrease with depth is defined through Beers law as Eq. (4):

$$K_{PAR} = -\ln(E_z/E_s)/z, \quad (4)$$

where K_{PAR} is the diffuse attenuation coefficient for PAR expressed in units of m^{-1}, E_z is the irradiance at depth z and E_s is the irradiance just below the water surface (Jerlov, 1976).

METHODS

Satellite Data Processing

The AVHRR data sets originated from the NOAA CoastWatch Program (Leshkevich et al., 1993), or were processed at the United States Geological Service (USGS) from raw data provided by the Earth Scan Lab at Louisiana State University. Thirteen NOAA-11 scenes, providing afternoon coverage, were processed to a Mercator projection with a pixel size of 1.06 km at 35°N. Imagery of visible (Channel 1, 580–680 nm) and near-infrared (Channel 2, 720–1000 nm) reflectance was used. The median value of a 3×3 pixel block was used for analysis against contemporaneous *in situ* measurements at each station, with the range of reflectances within the 3×3 block providing some estimate of spatial variability relative to the subpixel level (Stumpf and Pennock, 1989; Stumpf and Frayer, 1997). A Marquardt method of least squares approximation for nonlinear equations was used for fitting the plots. Clouds were masked using thresholds from Channel 2 and sea surface temperature (SST). Pixels contaminated by land were not included in the analysis.

Atmospherically corrected reflectance values, R_d, were derived from the satellite imagery and correlated with *in situ* K_{PAR} values following methods of Stumpf (1992) and Stumpf and Pennock (1989), applying the approach of Gordon et al. (1983). The aerosol correction at each pixel was obtained through the reflectance difference [Eq. (5)]

$$R_d = R(1) - R(2), \quad (5)$$

where R_d is the reflectance difference, a surrogate for R_w (Channel 1, 630 nm), and $R(1)$ and $R(2)$ are reflectances from Channels 1 and 2. This aerosol correction is effective because $R_w(2) << R_w(1)$ due to water absorption in Channel (2), although $R_w(2)$ is not always zero in turbid coastal water. Reflectance is determined as in Eq. (6):

$$R(\lambda) = \frac{\pi}{E_0(\lambda)} \frac{L_s(\lambda) - L_r(\lambda)}{(1/r^2)\, T_0(\lambda)\, T_1(\lambda) \cos\theta_0}, \quad (6)$$

where L_s is the radiance at the spacecraft, L_r is the Rayleigh radiance, E_0 is the extraterrestrial solar irradiance, r is the normalized Earth–Sun distance, and θ_0 is the solar zenith angle [see Eq. (3)]. Transmission from Sun to

surface (T_0), and from surface to satellite (T_1), are represented as T_x, with Eq. (7):

$$T_x(\lambda)=\exp[-(\tau_r(\lambda)/2+\tau_g(\lambda))/\cos\,\theta_x], \quad (7)$$

where τ_r is the Raleigh optical depth, τ_g is the gaseous absorption optical depth, θ_x represents the solar zenith angle (θ_0) or satellite angle (θ_1), respectively. Prelaunch calibrations were used for this study. Unlike other AVHRR sensors, NOAA-11 showed negligible degradation over its life (Rao and Chen, 1995; Teillet and Holben, 1994). Under extreme aerosol conditions, not all aerosols can be removed; therefore images with residual aerosol variability in clear (near offshore) water of R_d>0.003 were not used in the validation. This reduced the number of images from 13 to 10 for the final validation.

In Situ Data Collection

In situ data were collected concurrently with NOAA-11 AVHRR satellite overpasses on 13 dates between 1991 and 1993, with additional *in situ* optical data collected in 1994 (when NOAA-11 was not operating). Data were collected between April and November to take advantage of higher solar elevation angles during the satellite overpass. Twenty-six stations were sampled within 3 h of an overpass (Fig. 1). Stations were grouped into three geographic regions for analytical purposes: Pamlico River–5 uppermost river stations, Neuse River—10 uppermost river stations, and Pamlico Sound—11 stations. Sampling was conducted on days having relatively clear skies and a sea state <0.5 m.

The diffuse light attenuation coefficient, K_{PAR}, was determined from measurements of integrated irradiance between 400 nm and 700 nm, taken with a LiCor LI193-SA spherical quantum sensor coupled to a LiCor LI-1000 data logger. Two replicate profiles of scalar irradiance were taken at 0.5 m intervals between 0.5 m and 3.0 m. K_{PAR} was determined from linear regression of log-transformed irradiance measurements against depth. Irradiance data were log-transformed since decrease in irradiance with depth is approximately exponential. For calibration purposes, only values of K_{PAR} with an r^2>0.97 were used. Ninety-four percent of all *in situ* K_{PAR} data collected were acceptable based on these criteria.

At each station, surface water samples (<0.5 m depth) were collected and kept on ice for subsequent analyses of chlorophyll-*a* concentration, dissolved organic matter absorption (CDOM), and suspended sediment concentration. Chlorophyll-*a* was determined spectrophotometrically on Whatman 934 AH filtered material using the trichromatic method (Parsons et al., 1984). Suspended sediment concentrations were determined by filtering samples onto pretared Whatman GF/C filters, drying, and gravimetrically determining the weight gain of the filters. CDOM absorption, $a_{y(400\ nm)}$, was measured spectrophotometrically on filtered samples (GF/C filters) at 400 nm in a 5-cm cell against a distilled deionized water reference. Measured absorbance was converted (base *e*) to an absorption coefficient (m^{-1}).

In 1994, using an LI-1800UW submersible spectroradiometer (LI-COR, Inc.), 10 replicate spectral profiles of downwelling irradiance and five profiles of upwelling irradiance were averaged from 1 m depth at four stations (circled in Fig. 1), representing the widest range of optical variability. *In situ* spectral reflectance $R_w(\lambda)$ was calculated as E_u (upwelling irradiance)/E_d (downwelling irradiance). All measurements were taken within 3 h of solar noon from the sunny side of a boat. Data were collected under calm, cloud-free conditions. Errors can occur in measurement of upward irradiance by self-shading of the instrument (Gordon and Ding, 1992); hence reflectance calculations reported may be conservative or slight underestimates of actual values. Water samples were collected at the same depth and analyzed as above with the following exceptions: all samples (chlorophyll, CDOM, suspended sediments) were filtered through GF/F filters (effective filtration size approximately 0.7 μm) and chlorophyll *a* was analyzed using fluorometric techniques described by Parsons et al. (1984).

The total absorption coefficient, $a_t(\lambda)$ is wavelength-dependent and can be expressed as Eq. (8):

$$a_t(\lambda)=a_w(\lambda)+a_y(\lambda)+a_d(\lambda)+a_{ph}(\lambda), \quad (8)$$

where $a_w(\lambda)$ is absorption by pure water, $a_y(\lambda)$ is dissolved organic matter, $a_d(\lambda)$ is organic and inorganic detritus, and $a_{ph}(\lambda)$ is phytoplankton (Prieur and Sathyendranath, 1981). Spectral absorption was determined by first separating 1-m depth whole-water samples by filtration onto 25-mm Whatman GF/F filters. Both filtrate and filters were scanned between 400 nm and 750 nm at 1 nm intervals in a Perkin-Elmer Lambda 6 spectrophotometer. Sample and blank filters were saturated with distilled water just before scanning and placed on a plexiglass sheet in front of the detector with the sample side of the filter facing the light source. A scan of two wet blank filters were used for a baseline correction and residual absorbance at 750 nm was subtracted from all wavelengths (Kishino et al., 1985). To correct for increased pathlength due to multiple scattering in the glass-fiber filters, a quadratic relationship developed by Cleveland and Weidemann (1993) was used to estimate the optical density of the original suspension from the measured optical density of the filter. Absorption coefficient spectra were calculated from the suspension density, incorporating the volume filtered and the filter area (Mitchell, 1990). Total particulate matter absorption a_p was determined from scans of whole water sample filters. The filters were extracted twice in methanol, first for 1–3 h, then for 30 min, then rehydrated and scanned to determine a_d. Phytoplankton absorbance a_{ph} was determined as the difference of a_d from a_p (Kishino et al. 1985; 1986).

Table 1. Summary (Mean Value and Range) of Water Quality Parameters by Geographic Region for 13 Satellite Calibration Dates between 1991 and 1993

	Pamlico Sound				*Neuse River*				*Pamlico River*			
Water Quality Parameter	*n*	*min*	*max*	*mean*	*n*	*min*	*max*	*mean*	*n*	*min*	*max*	*mean*
Salinity (ppt)	99	8.9	23.7	18.5	126	0.3	21.8	11.7	54	0.7	18.5	10.3
K_{PAR} (m^{-1})	98	0.53	2.74	1.02	113	0.7	2.87	1.29	52	0.7	2.43	1.21
Secchi depth (m)	99	0.4	2.30	1.37	129	0.6	2.00	1.17	54	0.60	1.80	1.22
TSS (mg/L)	72	3.8	32.9	10.0	83	3.5	19.7	7.3	39	2.9	18.2	7.5
Chlorophyll (μg/L)	99	0.6	14.1	3.63	126	0.7	45.9	7.6	54	1.01	27.9	8.6
Dissolved organics (a m^{-1}, 400 nm)	99	0.5	5.0	1.9	129	1.3	14.9	4.4	52	2.0	12.7	4.1

RESULTS

Spatial Distribution of Optical Water Quality Parameters

In our study area, the locations of freshwater sources (Pamlico and Neuse Rivers) relative to coastal ocean inlets contributed to a general increase in salinity from west to east (Fig. 1) with mean surface salinities highest in Pamlico Sound (mean=18.5 %) (Table 1). Water quality data plotted against salinity show direct and inverse relationships with salinity (Fig. 2). Colored dissolved organic matter (CDOM), primarily humic substances of vascular plant origin from low-lying wetlands and coastal marshes (Moran et al., 1991; Moran and Hodson, 1994) was higher in the rivers and decreased steadily into the Sound (Pearson correlation coefficient $r=-0.77$, $p\leq 0.0001$, Fig. 2a). Above approximately 5‰ this decrease is likely due to dilution by offshore water, and below that to precipitation and settling of humic material coming into contact with saline water (Wells and Kim, 1989; Kirk, 1994).

Chlorophyll concentration was generally higher in the rivers than the Sound ($r=-0.49$, $p\leq 0.0001$) (Fig. 2b, Table 1); however, river concentrations varied more over time, as evidenced by the increased scatter of data in the lower salinity range. The Neuse River estuary is sensitive to excessive nutrient loading and responds to seasonal hydrological cycles and short-term meteorological events through shifts in phytoplankton community structure and biomass (Pinckney et al., 1998). Phytoplankton bloom formation is particularly evident from late winter through the summer months, yielding subsequent organic matter loads capable of causing extensive hypoxic and anoxic conditions in the river (Paerl et al., 1998).

Total suspended sediment (TSS) concentration (Fig. 2c) showed two distinct distributions. With the exception of one sampling date (November 1992), no significant difference was evident between suspended sediment concentration in the rivers and the Sound ($r=-0.11$, $p=0.17$). There was a significant positive correlation between suspended sediments and salinity in November 1992 ($r=0.81$, $p\leq 0.0001$). Sampling occurred the day after a storm event, and as a result of wind resuspension of bottom sediments, a greater increase of TSS was observed in the Sound relative to the rivers. Pamlico Sound is relatively shallow with an approximate 100 km fetch. In these circumstances, winds can easily destratify the water column and resuspend bottom sediments through wave processes (Wells and Kim, 1989).

K_{PAR} was higher in the rivers compared to the Sound ($r=-0.66$, $p\leq 0.0001$) (Fig. 2d, Table 1). In the rivers, the increased absorption by CDOM and chlorophyll plausibly explains the increased K_{PAR}. Increased mean values of chlorophyll and CDOM were evident in the rivers compared to the Sound, while mean TSS concentration was slightly less in the rivers compared to the Sound (Table 1, Fig. 2). In addition, an increase in K_{PAR} was correlated to CDOM absorption ($r=0.61$, $p\leq 0.0001$), chlorophyll concentration ($r=0.45$, $p\leq 0.0001$), and to a lesser extent TSS concentration ($r=0.28$, $p\leq 0.0001$).

ALGORITHM APPLICATION

Mean K_{PAR} values ranged from 1.0 m^{-1} in Pamlico Sound ($n=98$) to 1.3 m^{-1} in the Pamlico and Neuse rivers ($n=165$). Using an effective remote sensing depth of 1 attenuation length (Gordon and McLuney, 1975), the radiance measured by the sensor originated from depths <1.0 m in the Sound and <0.8 m in the rivers. Based on this information, in our study area reflectance from the bottom is not an interference except within about 2 km of shore in the Sound and less than 1 km from shore in lower portions of the rivers.

K_{PAR} and TSS were linearly correlated in the main body of Pamlico Sound (Fig. 3), indicating a scattering-dominated system; accordingly, the application of Eq. (2) is appropriate in the Sound. The regression equation ($K_{PAR}=0.49+0.077*TSS$; $r^2=0.81$) fits the data for 12 dates sampled (Fig. 3). The slope of this line (0.077) is similar to that found in Delaware Bay (slope=0.074) (Stumpf and Pennock, 1991). A second equation fits data collected from November 1992 ($K_{PAR}=-0.97+0.086*TSS$; $r^2=0.94$), shortly after a storm event. We hypothesized that the increase in suspended sediment concentration on that date was due to resuspension from the bottom of larger diameter particles (i.e., fine sand) than are generally present in the water column. The scattering effi-

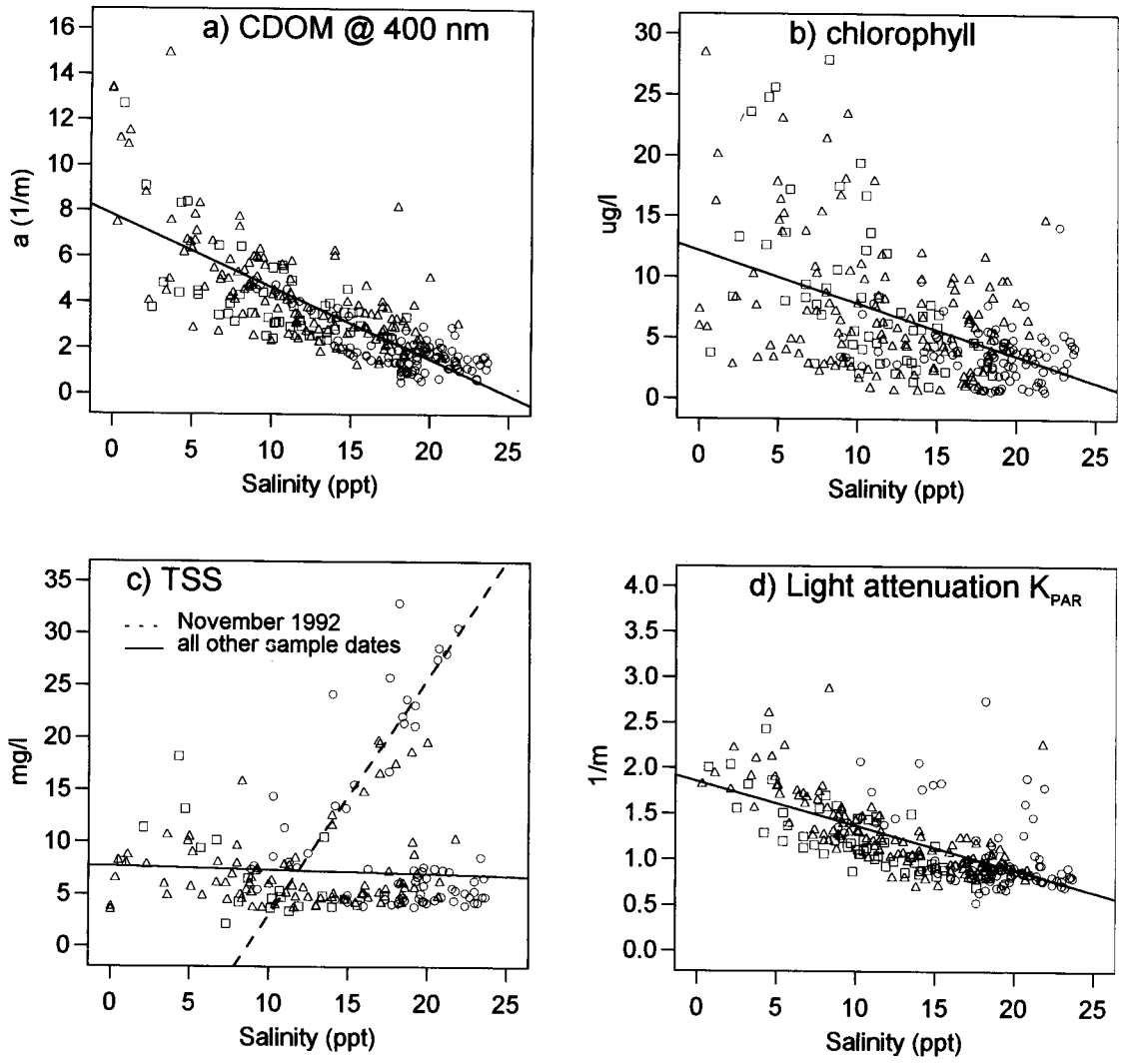

Figure 2. Salinity plotted against water quality data from dates of satellite overpasses: a) colored dissolved organic matter (CDOM), measured as an absorption coefficient (a m^{-1}) at 400 nm, b) chlorophyll (μg/L), c) TSS (mg/L), and d) light attenuation K_{PAR} (m^{-1}). Geographic locations are noted as Neuse River (△), Pamlico River (□), and Pamlico Sound (○).

ciency of optically active particles decreases as the ratio of particle volume to cross-sectional area is increased (Van de Hulst, 1957; Baker and LaVelle, 1984). Hence, larger diameter particles are less effective at scattering light for a given mass than smaller diameter particles. K_{PAR} from November 1992 is less than on all other sample dates, given the same TSS concentration, suggesting more efficient scattering by smaller particles (Fig. 3).

A similar relationship is shown between suspended sediments and satellite reflectance R_d (Fig. 4a). While sediment concentrations are greater in November, there is no corresponding increase in reflectance. We postulate that the relationship between K_{PAR} and satellite reflectance (R_d) is stable even if the sediment grainsize changes, since K_{PAR} and R_d are primarily dependent on the optical cross-sectional area (d^2) of particles. TSS, however, is a volumetric (d^3) relationship, so the R_d–TSS relationship would be sensitive to changes in grain size. Although the R_d–TSS data show clear separations by date (Fig. 4a), the R_d–K_{PAR} data (Fig. 4b) show November 1992 data overlapping the main body of data.

The overall relationship between R_d and K_{PAR} for Pamlico Sound is shown in Figure 4b, represented by Eq. (2) for 10 dates sampled, including November 1992. In the model over 72% of the variance of R_d can be explained by K_{PAR}. Superimposed on Figure 4b are the fitted equations for Mobile Bay (Stumpf and Pendygraft, 1997) and Delaware Bay (Stumpf and Pennock, 1991) using the same general model [Eq. (2)]. The Delaware Bay coefficients were converted to correct for differences in NOAA-9, and NOAA-11 calibrations are based on Rao and Chen (1995). Pamlico Sound and Mobile Bay show comparable results. Delaware Bay has a higher G coefficient relative to F (for $G/K_{PAR} >> 1$, the ratio of F/G

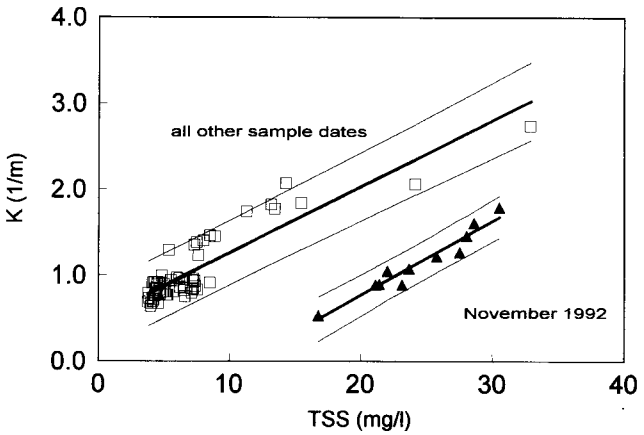

Figure 3. K_{PAR} (m^{-1}) vs. TSS (mg/L) in Pamlico Sound for 12 satellite calibration dates (□), and November 1992 calibration date (▲) after a recent storm.

is important as Eq. (2) tends toward $R_d = Y'(F/G)K_{PAR}$ compared to Pamlico Sound or Mobile Bay, suggesting slightly more absorption in that estuary (Table 2).

Although G in Eq. (2) permits some correction for absorption, with only one broad band in the visible region the AVHRR cannot be used to discriminate between several sources of moderate to high absorption (i.e., organic matter and phytoplankton pigments), as is present in our study area. K_{PAR} was dominated by suspended sediment (scattering) processes in the Sound, which allowed development of the R_d–K_{PAR} algorithm; however, the rivers were dominated by absorption of consistently high levels of organic matter and periodic elevated concentrations of phytoplankton pigments. The high backscatter occurring in the rivers indicates that significant reflectance occurs in the near-IR band used for atmospheric corrections. R_d becomes low owing to high absorption in Band 1 (630 nm) and overcorrection for the atmosphere, frequently falling below a useful detection (R_d<0.01) in the rivers. Therefore, data from the 10 Neuse River and five Pamlico River stations were not used in the final algorithm development.

Using our generalized model of Pamlico Sound to determine K_{PAR} (i.e., for the 10 dates sampled), 66% of the variance in the data was explained at the 95% confidence level (Fig. 5). When sampling date is included in the model as a variable, 86% of the variance is explained. The remaining variance not explained by the model has several possible sources including subpixel variability, and the relatively modest range of data available for development of the model. The November 1992 data fall within the 95% confidence interval of the model indicating the equation estimating attenuation (Fig. 4b) is more robust than the equation for reflectance and suspended sediment concentration (Fig. 4a) under varying meteorological conditions, although extrapolation of Eq. (2) beyond the ranges of the data set is not advised.

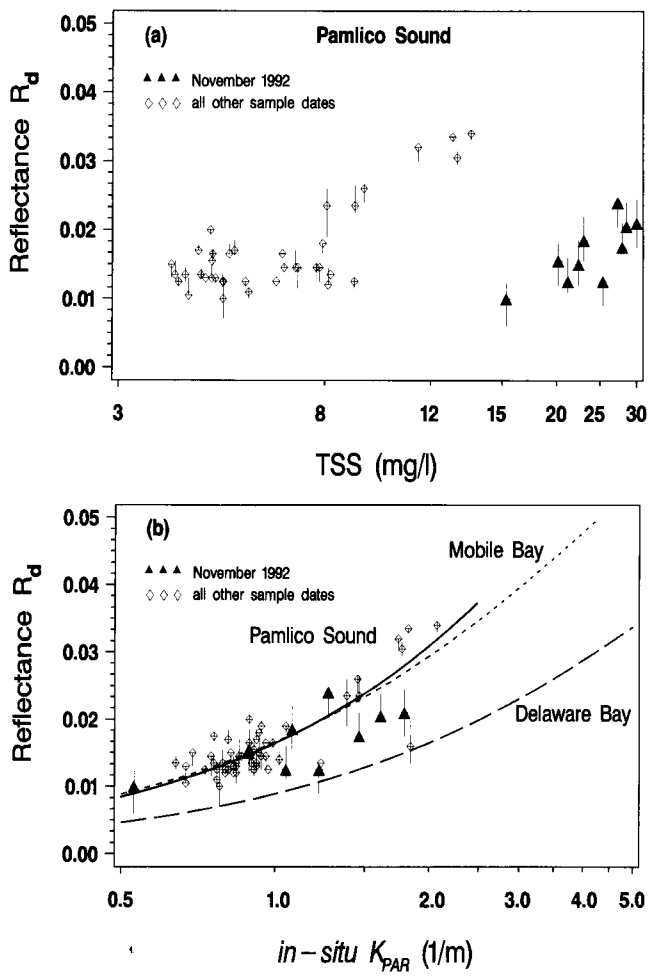

Figure 4. AVHRR reflectance (R_d) plotted against a) TSS (mg/L), and b) *in situ* K_{PAR} (m^{-1}) with fitted equation $R_d = 0.178 * F/(1+G/K)$ for Pamlico Sound, where $F=1.46$ and $G=14.79$. Fitted equations for Mobile Bay (– – –) (Stumpf and Pendygraft, 1997) and Delaware Bay (— — —) (Stumpf and Pennock, 1991) are shown also. R_d has been aerosol corrected [Eq. (7)]. Error bars show the range of a 3×3 pixel block with median plotted.

The impact of absorption on remotely-sensed reflectance in the rivers is quite apparent (Fig. 6a), as shown by the extremely low R_d values in the rivers. Although reflectance is reduced in the river, K_{PAR} is increasing, due to the additive effects of CDOM, chlorophyll, and suspended sediment contributions to increased light attenuation. Therefore, the algorithm for determining K_{PAR} is valid only in the main body of Pamlico Sound. Channel 1 reflectances decrease relative to Channel 2 in the rivers primarily because of high absorption by DOM and chlorophyll. This phenomenon does not result from proximity to land as shown by Stumpf and Tyler (1988). The reduction is partially due to an artifact of the aerosol correction [Eq. (5)], where Channel 2 is subtracted from Channel 1 to remove atmospheric haze. Channel 2 contains some reflectance from the water due to scattering

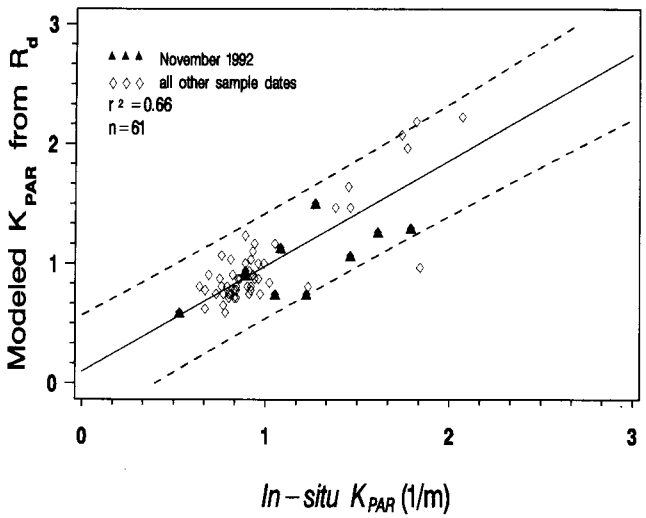

Figure 5. *In situ* K_{PAR} (m^{-1}) plotted against modeled K_{PAR} (m^{-1}) from R_d for Pamlico Sound. Dashed line represents 95% confidence interval of the regression.

material; thus subtraction may artificially reduce the estimated reflectance.

The strong variations in absorption can be identified from AVHRR imagery using a color index (C_{21}) on days having fairly clear homogenous atmospheric conditions. The color index is represented as Eq. (9):

$$C_{21}=\frac{R(2)-R_a(2)}{R(1)-R_a(1)}, \qquad (9)$$

where R is reflectance with Rayleigh scattering removed and R_a is the aerosol component, estimated as reflectance over clear near-offshore waters (Stumpf and Tyler, 1988). C_{21} varies approximately linearly with absorption in Channel 1 and has been shown to correspond to the presence of algal blooms (Stumpf and Tyler, 1988; Gower, 1994). C_{21} in the clearest coastal waters is ~0.10 (Gower, 1994) increasing to 0.3 in blooms off the west coast of Canada, and >1.0 in some 80 μg/L blooms in Chesapeake Bay (Stumpf and Tyler, 1988). Figure 6b shows a strong increase in C_{21} in the rivers (>1.0) relative to Pamlico Sound (<0.5). Higher C_{21} values in our region are due to a combination of CDOM, phytoplankton pigments, and detrital absorption, as shown by spectrally averaged absorption coefficients (580–680 nm, Table 3), decreasing $R(1)$ relative to $R(2)$. C_{21} differences between the rivers (1–1.4) and Pamlico Sound (0.3–0.4) agree with the almost three times increase in a_t (580–680 nm) seen in the upper river compared to the Sound (Table 3). In Eq. (2), G is a constant which includes an absorption term for both chlorophyll and dissolved organics. If absorption at Channel 1 wavelength varies, then G would change accordingly. In Figure 6b absorption in Channel 1 varies in our study area, with the greatest change occurring between the rivers and the Sound. In Pamlico Sound C_{21} is relatively constant; therefore, G remains constant in this region for purposes of a general algorithm application.

Khorram and Cheshire (1985) used Landsat MSS in the Neuse River to estimate salinity, chlorophyll, turbidity (NTU), and TSS using statistically derived regression equations in the Neuse River estuary. Coefficients of determination (r^2) for remotely sensed reflectance were highest for salinity (0.82) compared to other variables measured. In theory, salinity cannot be remotely sensed directly with Landsat MSS. However, salinity may be acting as a surrogate for dissolved organic matter which is optically active, and the high r^2 value Khorram and Cheshire (1985) observed between reflectance and salinity may be attributable to a strong relationship between salinity and organic matter.

In situ spectral signatures in our study area provided a means of understanding how absorption and scattering properties change with wavelength, thereby influencing remotely sensed reflectance. Reflectance spectra are a combined function of absorption and scattering properties from dissolved organic matter, phytoplankton, suspended particulates, and water. As an example, spectral signatures from the same date as absorption coefficient data (Table 3) show the greatest spectral reflectance in Pamlico Sound followed by decreasing reflectance at the Neuse River stations progressing upstream in the river (Fig. 7). Total integrated *in situ* reflectance (400–700 nm) is greatest in Pamlico Sound, even though K_{PAR} is less in the Sound (1.46 m^{-1}) than in the upper Neuse River (1.78 m^{-1}), indicating the increased influence of scattering processes in the Sound relative to the rivers.

The reflectance signatures (Fig. 7) are similar to those found in other highly colored, turbid inland and coastal waters (Dekker et al., 1992; Kirk, 1994). Decreased reflectance is apparent between 400 nm and 500 nm due to combined absorption by phytoplankton pigments, DOM, and detritus. Reflectance increases up to 580 nm as a result of lower absorption by pigments and DOM, coupled with greater scattering by particulates. Reduced relative reflectance around 630 nm is due to phycocyanin absorption by blue green algae. A second chlorophyll *a* absorption band is visible at 675 nm. The wavelength region encompassed by the AVHRR Channel 1 band includes the shoulder of maximum reflectance (580–600 nm), two pigment absorption bands (phycocyanin and chlorophyll *a*), and overall absorption effects from CDOM, providing useful information for correlation with K_{PAR}. While ocean color sensors are designed to extract the most meaningful information in the blue to green wavelength regions, the AVHRR is appropriately suited to extract useful information from turbid coastal regions in the red and near-infrared regions.

CONCLUSIONS

The relationship between reflectance in the red region (580–680 nm) and K_{PAR} in Pamlico Sound is fairly robust

(r^2=0.72) under varying environmental conditions, including changes in sediment optical characteristics such as grain size, while the relationship between R_d and suspended sediment concentration is affected by changing sediment characteristics, making development of a general equation more problematic. For longer term data sets, an estimation of K_{PAR} may provide a more consistent measure of turbidity, in addition to its biological relevance for productivity studies. The close match between R_d–K algorithms developed for Pamlico Sound, Delaware Bay (Stumpf and Pennock, 1991), and Mobile Bay (Stumpf and Pendygraft, 1997) is promising for future development of regional algorithms for K_{PAR} of coastal bays and estuaries with generally similar sediment types. In areas where suspended sediment concentrations already exist, reflectance data may provide additional information regarding changes in sediment grain size and other optical characteristics. The similarities between dif-

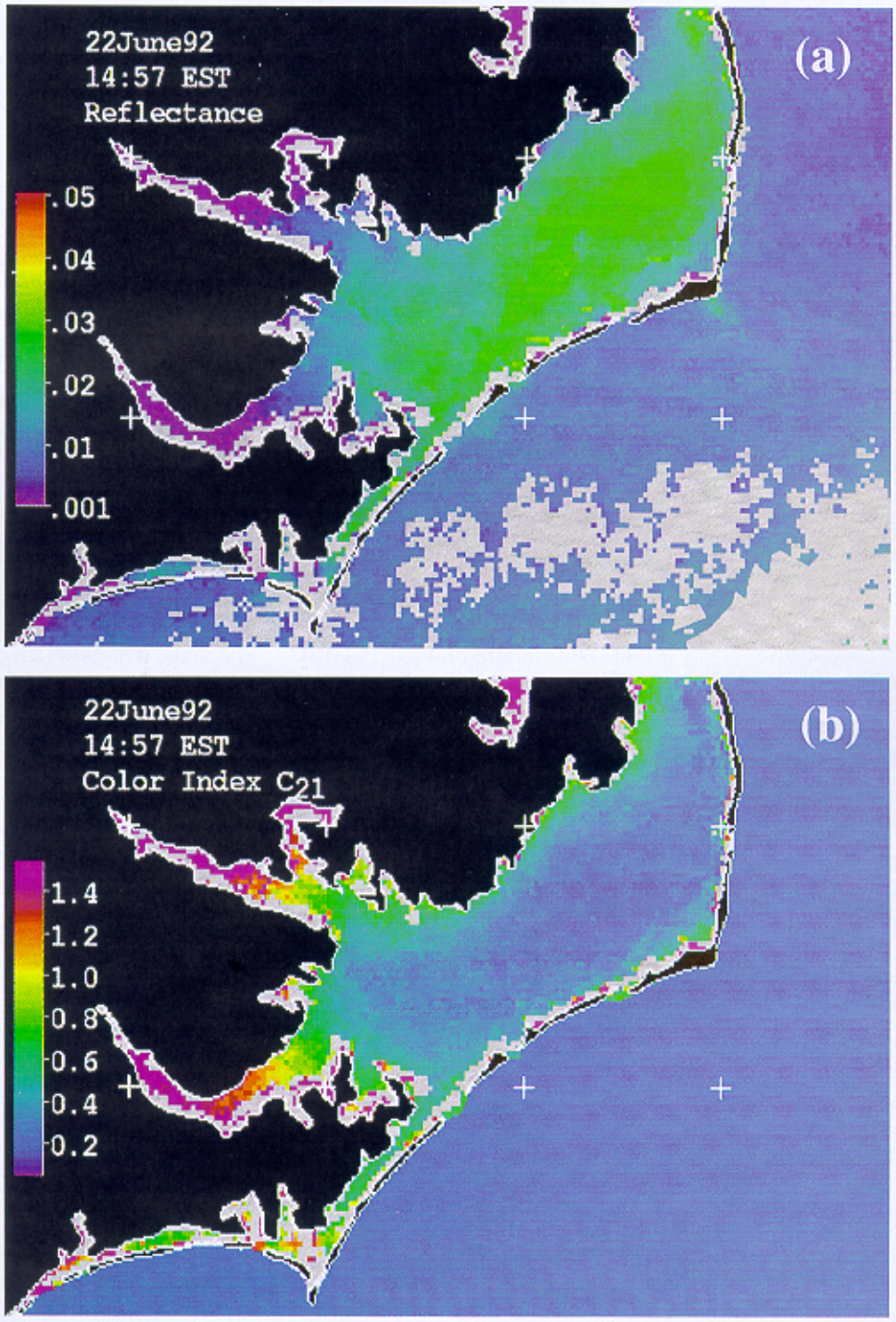

Figure 6. a) Atmospherically corrected reflectance (R_d) from NOAA-11 AVHRR in Pamlico Sound and the lower Neuse and Pamlico rivers, 22 June 1992. R_d color bar and scale applies to entire study area. In Pamlico Sound only, R_d of 0.01, 0.02, 0.03, 0.04, and 0.05 corresponds to K_{PAR} of 0.6 m^{-1}, 1.2 m^{-1}, 1.9 m^{-1}, 2.7 m^{-1}, and 3.5 m^{-1}, respectively. b) Color index (C_{21}) in Pamlico Sound and tributaries from NOAA-11 AVHRR, 22 June 1992. The Atlantic ocean has been masked to eliminate clear water areas where the color index is inappropriate.

Table 2. Sediment (F) and Absorption (G) Coefficients Determined for Eq. (3)

Geographic Area	*AVHRR Sensor*	F	G	n	r^2
Pamlico Sound[a]	NOAA-11	1.46	14.79	61	0.72
Delaware Bay[b]	NOAA-9	0.63	11.6	16	0.84
Mobile Bay[c]	NOAA-10/11	0.72	6.71	113	0.76

[a] This study.
[b] Stumpf and Pennock (1991).
[c] Stumpf and Pendygraft (1997).

Table 3. Spectrally Averaged Absorption Coefficients (m^{-1}) for Wavelengths of K (400–700 nm) and AVHRR Channel 1 (580–680 nm)[a]

	400–700 nm		*580–680 nm*	
	Upper Neuse River	*Pamlico Sound*	*Upper Neuse River*	*Pamlico Sound*
Particulate (a_p)	2.92	0.41	0.99	0.14
Detritus (a_d)	1.36	0.39	0.29	0.10
Phytoplankton (a_{ph})	1.55	0.01	0.70	0.04
Dissolved organics (a_y)	2.26	0.64	0.95	0.40
Pure water (a_w)	0.16	0.16	0.30	0.30
Total (a_t)	5.33	1.21	2.25	0.84

[a] Example taken at 1 m depth from the upper Neuse River station and Pamlico Sound station (circled in Fig. 1) on 3 November 1994.

ferent regions may allow us to interpret higher R_d values than observed here. By sampling under calm conditions, a necessity for adequate calibration of the satellite, rather than during storm events which would tend to increase turbid conditions, we were acquiring a relatively narrow range of K_{PAR} values in our calibration data set. In the future, stationary buoys acquiring continuous data would greatly increase the probability of extending the range of K_{PAR} data for calibration purposes.

SeaWiFS Band 6 (660–680 nm) resembles AVHRR Band 1 at 580–680 nm, owing to the relatively high influence of water absorption in both bands. This suggests that we can transfer the relationship to Band 6 after providing for some intersatellite comparisons. Determination of K_{PAR} in optically complex coastal waters such as the Neuse River, will remain problematic even with the SeaWiFS sensor. SeaWiFS has the potential to estimate the absorption through various solutions which can be incorporated into the model through adjustment of the coefficients. The AVHRR will provide historical continuity between CZCS (operational until 1986), SeaWiFS, and future sensors. With continued daily coverage provided by AVHRR, this sensor should complement future ocean color studies.

Figure 7. Example of *in situ* reflectance plotted as a function of wavelength. Samples taken at 1 m depth, 3 November 1994 from the four stations circled in Figure 1. Dashed vertical lines represent the 580–680 nm AVHRR bandwidth.

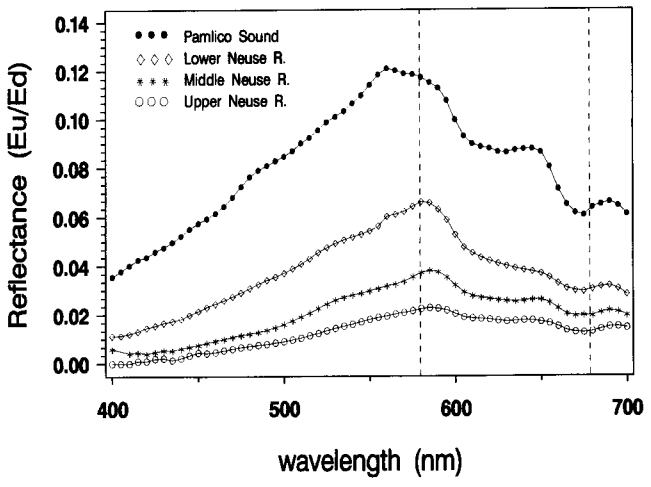

We would like to thank M. Mallin, M. Go, H. Walsh, W. Hettler, and numerous others for assistance in the field and laboratory, R. Ferguson and D. Colby for valued input related to experimental design and statistical analyses, and P. Whitfield for graphics design. We thank A. Chester, J. Pinckney, and W. Hettler for helpful comments on early versions of the manuscript, and comments by several anonymous reviewers which significantly improved the article. This research was supported by a grant from NOAA's Coastal Ocean Program through Coast-Watch to the National Marine Fisheries Service in Beaufort, North Carolina.

REFERENCES

Austin, R. W., and Petzold, T. J. (1981), Water Colour Measurements. In *Oceanography from Space* (J. F. R. Gower, Ed.), Plenum, New York, pp. 239–256.

Baker, E. T., and LaVelle, J. W. (1984), The effect of particle

size on the light attenuation coefficient of natural suspensions. *J. Geophys. Res.* 89(C5):8197–8203.

Carder, K. L., and Steward, R. G. (1985), A remote-sensing reflectance model of a red-tide dinoflagellate off west Florida. *Limnol. Oceanogr.* 30:286–298.

Cleveland, J. S., and Weidemann, A. D. (1993), Quantifying absorption by aquatic particles: a multiple scattering correction for glass-fiber filters. *Limnol. Oceanogr.* 38(6):1321–1327.

Copeland, B. J., and Gray, J. (1989), *Albemarle–Pamlico Estuarine System: Preliminary Technical Analysis of Status and Trends*, Albemarle–Pamlico Study Report 89-13A, North Carolina Department of Environmental Health and Natural Resources, Raleigh.

Dekker, A. G., Malthus, T. J., Wijnen, M. M., and Seyhan, E. (1992), Remote sensing as a tool for assessing water quality in Loosdrecht lakes. *Hydrobiologia* 233:137–159.

Epperly, S. P., and Ross, S. W. (1986), *Characterization of the North Carolina Pamlico–Albemarle Estuarine Complex*, NOAA Technical Memorandum NMFS-175, Beaufort, NC.

Gordon, H. R., and McLuney, W. R. (1975), Estimation of the depth of sunlight penetration in the sea for remote sensing. *Appl. Opt.* 14:413–416.

Gordon, H. R., and Morel, A. Y. (1983), *Remote Assessment of Ocean Colour for Interpretation of Satellite Visible Imagery. A Review*,Springer-Verlag, New York.

Gordon, H. R., and Ding, K. (1992), Self-shading of in-water optical instruments. *Limnol. Oceanogr.* 37:491–500.

Gordon, H. R., Brown, O. B., and Jacobs, M. M. (1975), Computed relationships between the inherent and apparent optical properties of a flat homogenous ocean. *Appl. Opt.* 14:417–427.

Gordon, H. R., Clark, D. K., Brown, J. W., Brown, O. B., Evans, R. H., and Broenkow, W. W. (1983), Phytoplankton pigment concentrations in the Middle Atlantic Bight: comparison of ship determinations and CZCS estimates. *Appl. Opt.* 22:20–36.

Gould, R. W., Jr., and Arnone, R. W. (1997), Estimating the beam attenuation coefficient in coastal waters from AVHRR imagery. *Remote Sens. Environ.* 17:1375–1387.

Gower, J. F. R. (1994), Red tide monitoring using AVHRR HRPT imagery from a local receiver. *Remote Sens. Environ.* 48:309–318.

Jerlov, N. J. (1976), *Marine Optics*, Elsevier, Amsterdam.

Khorram, S. (1985), Development of water quality models applicable throughout the entire San Francisco Bay and Delta. *Photogramm. Eng. Remote Sens.* 51:53–62.

Khorram, S., and Cheshire, H. M. (1985), Remote sensing of water quality in the Neuse River Estuary, North Carolina. *Photogramm. Eng. Remote Sens.* 51:329–341.

Kirk, J. T. O. (1994), *Light and Photosynthesis in Aquatic Systems*, 2nd ed., Cambridge University Press, Cambridge.

Kishino, M., Takahashi, M., Okami, N., and Ichimura, S. (1985), Estimation of the spectral absorption coefficients of phytoplankton in the sea. *Bull. Mar. Sci.* 37:634–642.

Kishino, M., Okami, N., Takahashi, M., and Ichimura, S. (1986), Light utilization efficiency and quantum yield of phytoplankton in a thermally stratified sea. *Limnol. Oceanogr.* 31:557–566.

Leshkevich, G. A., Schwab, D. J., and Muhr, G. C. (1993), Satellite environmental monitoring of the Great Lakes: a review of NOAA's Great Lakes CoastWatch program. *Photogramm. Eng. Remote Sens.* 59:371–379.

Mallin, M. A., Paerl, H. W., and Rudek, J. (1991), Seasonal phytoplankton composition, productivity, and biomass in the Neuse River Estuary, NC. *Estuar. Coast. Shelf Sci.* 32:609–623.

Mitchell, B. G. (1990), Algorithms for determining the absorption coefficient for aquatic particulates using the quantitative filter technique. In *Ocean Optics 10*, Proc. SPIE 1302, pp. 137–148.

Moran, M. A. and Hodson, R. E. (1994), Dissolved humic substances of vascular plant origin in a coastal marine environment. *Limnol. Oceanogr.* 39:762–771.

Moran, M. A., Pomeroy, L. R., Sheppard, E. S., Atkinson, L. P.,and Hodson, R E. (1991), Distribution of terrestrially derived dissolved organic matter on the southeastern U.S. continental shelf. *Limnol. Oceanogr.* 36:1134–1149.

Morel, A. (1988), Optical modeling of the upper ocean in relation to its biogenous matter content (Case I waters). *J. Geophys. Res.* 93:10,749–10,768.

Morel, A., and Gentili, B. (1993), Diffuse reflectance of oceanic waters: bidirectional aspects. *Appl. Opt.* 32:6864–6879.

Morel, A., and Prieur, L. (1977), Analysis of variations in ocean color. *Limnol. Oceanogr.* 22:709–722.

Morel, A., Voss, K. J., and Gentili, B. (1995), Bidirectional reflectance of oceanic waters: a comparison of modeled and measured upward radiance fields. *J. Geophys. Res.* 100(C7): 13,143–13,150.

Paerl, H. W., Mallin, M. A., Donahue, C. A., Go, M., and Peierls, B. L. (1995), *Nitrogen Loading Sources and Eutrophication of the Neuse River Estuary, North, Carolina: Direct and Indirect Roles of Atmospheric Deposition*, Water Resources Research Institute, Report No. 95-291, University of North Carolina, Raleigh.

Paerl, H. W., Pinckney, J. L., Fear, J. M., and Peierls, B. L. (1998), Ecosystem responses to internal and watershed organic matter loading: consequences for hypoxia in the eutrophying Neuse River Estuary, North Carolina, USA. *Mar. Ecol. Prig. Ser.* 166:17–25.

Parsons, T. R., Maita, Y., and Lalli, C. M. (1984), *A Manual of Chemical and Biological Methods for Seawater Analysis*, Pergamon, New York.

Pennock, J. R. (1985), Chlorophyll distributions in the Delaware Estuary: regulation by light-limitation. *Estuar. Coast. Shelf Sci.* 21:711–725.

Pinckney, J. L., Paerl, H. W., Harrington, M. B., and Howe, K. E. (1998), Annual cycles of phytoplankton community-structure and bloom dynamics in the Neuse River Estuary, North Carolina. *Mar. Biol.* 131:371–381.

Platt, T., Caverhill, C., and Sathyendranath, S. (1991) Basin-scale estimates of oceanic primary production by remote sensing: the North Atlantic. *J. Geophys. Res.* 96:15,147–15,161.

Prieur, L., and Sathyendranath, S. (1981), An optical classification of coastal and oceanic waters based on the specific spectral absorption curves of phytoplankton pigments, dissolved organic matter, and other particulate materials. *Limnol. Oceanogr.* 26:671–689.

Rao, C. R. N., and Chen, J. (1995), Post-launch calibration of the visible and near-infrared channels of the Advanced Very High Resolution Radiometer on the NOAA-14 spacecraft. *Int. J. Remote Sens.* 17:2743–2747.

Smith, R. C., and Baker, K. S. (1978), The bio-optical state of ocean waters and remote sensing. *Limnol. Oceanogr.* 23:247–259.

Spinrad, R. (1989), Hydrologic optics. *Limnol. Oceanogr.* 34:1389–1766.

Stumpf, R. P. (1992), Remote sensing of water clarity and suspended sediments in coastal waters. In *Proceedings of the First Thematic Conference on Remote Sensing for Marine and Coastal Environments*, SPIE 1930, pp. 293–306. New Orleans, LA.

Stumpf, R. P., and Frayer, M. L. (1997), Temporal and spatial change in coastal ecosystems using remote sensing: Example with Florida Bay, USA, emphasizing AVHRR imagery. In *Proceedings of the Fourth International Conference on Remote Sensing for Marine and Coastal Environments*, ERIM Vol. I, pp. 65–74. Orlando, FL.

Stumpf, R. P., and Pendygraft, S. L. (1997) *Satellite Imagery of the North-Central Gulf of Mexico and Mobile Bay, Alabama, December 1989–May 1993*, U.S. Geological Survey, Digital Data Series, Reston, VA.

Stumpf, R. P., and Pennock, J. R. (1989), Calibration of a general optical equation for remote sensing of suspended sediments in a moderately turbid estuary. *J. Geophys. Res.* 94(C10):14,363–14,371.

Stumpf, R. P., and Pennock, J. R. (1991), Remote estimation of the diffuse attenuation coefficient in a moderately turbid estuary. *Remote Sens. Environ.* 38:183–191.

Stumpf, R. P., and Tyler, M. A. (1988), Satellite detection of bloom and pigment distributions in estuaries. *Remote Sens. Environ.* 24:385–404.

Teillet, P. M., and Holben, B. N. (1994), Towards operational radiometric calibration of NOAA AVHRR imagery in the visible and near-infrared channels. *Can. J. Remote Sens.* 20:1–10.

Van de Hulst, H. C. (1957), *Light Scattering by Small Particles*, Wiley, New York.

Wells, J. T., and Kim, S. Y. (1989) Sedimentation in the Albemarle–Pamlico Lagoonal System: synthesis and hypotheses. *Mar. Geol.* 88:263–284.

Whitlock, C. H., Poole, L. R., Usry, J. W., et al. (1981), Comparison of reflectance with backscatter and absorption parameters for turbid waters. *Appl. Opt.* 20:517–522.